TechnoChem

International Journal of TechnoChem Research
ISSN: 2395-4248 www.technochemsai.com
Vol.01, No.01, pp 35-49, 2015

# A Review on Hydrodynamics of Gas Inducing Mechanically Agitated Contactors.

**Eldho Abraham**

**Department of Chemical Engineering, St. Joseph's College of Engineering, Chennai, India.**

**Abstract :** In this paper an effort has been made to review the renowned literatures in the area of gas inducing mechanically agitated contactors (GIMACs) and to summarize inferences. This work is done in a preceptorial focus of integrating technical information on hydrodynamics of GIMACs wide spread through a large number of literatures of eminent authors. The classification and the air induction mechanism of the GIMACs were explained. The hydrodynamic models and correlations developed by various authors for single orifice impellers in terms of critical impeller speed, gas induction rate and power consumption were critically reviewed. The various extensions of the single orifice models to the multiple orifices models were also analyzed. Various equations those are involved in the estimation of the pressure driving force had also been discussed. Different regimes of gas bubble formation and bubble ejection were also explained along with the details of gas holdup, bubble size and bubble size distribution. Different correlations for finding the bubbles sizes under corresponding regimes were also dealt in this work.

**Key words**: GIMAC, gas inducing mechanically agitated contactor, impeller blade, gas induction, critical speed, power consumption, rate of gas induction, pressure driving force, gas holdup, bubble size.

## 1.Introduction

The Gas Inducing Mechanically Agitated Contactors (GIMACs) are gaining importance now a days because of their lower power consumption and more effective solute gas utilization as compared with the conventional gas sparging mechanically agitated contactors. The most outstanding feature of the gas inducing system is considered as its less dependence on the liquid fill level. The above features of the GIMAC can be effectively exploited in several industrially important chemical processes like hydrogenation, alkylation, ozonolysis, oxidation, hydrochlorination, ammonolysis, hydrobromination, addition halogenations etc. The special geometric features imparted to the rotor system in the form of a hollow shaft, gas passing channels through the impeller blades connecting to the hollow shaft and the orifices on the impeller blade surface creates the necessary gas pathway from the headspace to the impeller blade surface. In general the rotation of the impeller lowers the pressure in the liquid than the head space pressure and this makes the gas in the head space to flow through the gas pathway to the reactor liquid[1,6,9]. The mechanism of the gas induction is dealt in detail later in this paper. A typical gas inducing system is represented schematically in the figure 1.

### 1.1. Mechanism of gas induction

The mechanism of the gas induction has described in detail in many literatures [1,6,9]. Due to the hydrostatic equilibrium, the water level inside the hollow impeller equals with the water level in the tank when the impeller is in rest. Let P(θ) be the pressure acting over the orifice at any angular position due to the liquid static head and $P_o$ be the head space pressure. When the impeller starts to rotate, it imparts the necessary kinetic energy to the liquid, which creates a corresponding movement in the liquid. As a result the static pressure head

offered by the liquid gradually reduces with respect to the increase in impeller speed. At a particular point of liquid velocity, the pressure acting on any angular position of the orifice is reduced to a level which is lower than the head space pressure.

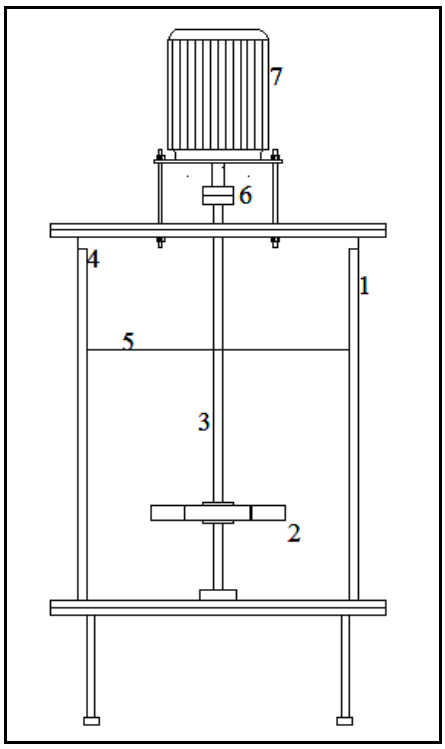


**Figure:1 Gas inducing mechanically agitated contactor**

1. Tank
2. Gas inducing impeller
3. Hollow shaft
4. Baffles
5. Liquid level
6. Coupling
7. Drive motor

Due to this pressure difference, the gas at the head space flows to the liquid through the hollow channel and this caused the gas induction. The beginning of the gas induction will be at a point when the $P_o$ equals the $P(\theta)$. The impeller speed at this instance is referred as critical impeller speed of the gas induction process. It has been found from the various literatures that the centrifugal force acting on the gas due to the impeller rotation have negligible effect on the gas induction. There is considerable pressure loss due to the flow gas through the hollow shaft, channel inside the impeller blade and the orifice due to frictional and orifice loss. In addition to this the exit of the gas from the orifice front to the working liquid in the form of bubbles also expends energy causing a drop in pressure[12,13]. These pressure drops together can be accounted as total pressure drop and can be denoted as $\Delta P_T$. The driving force for the gas induction through the orifice is the pressure difference between the head space pressure and the pressure acting on the orifice at any angular location. The gas induction occurs when the difference between the $P_o$ and the $P(\theta)$ slightly exceeds the value of $\Delta P_T$.

As far as the gas induction in a GIMAC as concern the hydrodynamics of the systems serves an important role and this deals with various systems behaviors like the pressure reduction in the liquid, critical gas induction speed, gas induction rate, power consumption, gas hold up, mechanism of gas bubble formation, ejection of the bubbles from the orifice, bubble size, residence time and distribution of the bubbles in the liquid etc. In addition to this, the various geometrical and non geometrical parameters of the system have a strong influence on these behaviors.

### 1.2. Classification of the GIMACs

Basically the GIMACs can be classified based on two criteria[1]. The first criterion is the interaction of the system head space to the surrounding. According to this the gas inducing systems are classified into open end systems and dead or closed end systems. The open end systems are the systems in which the solute gas is not readily available for the recycle as the system head space is open to the atmosphere. In most of these cases the gas induced will be atmospheric air and the recirculation of the solute gas can be expected only up to a certain extend. The dead end a system, as the head space is exists with a closed circuit which is not open to the atmosphere; the entire solute gas will be readily available for the recycling. In both the systems, the hydrodynamic behaviors are found more or less similar.

The second criterion is the input and output fluid flows. Based on this the systems can be classified into three types as given below[1].

1. The inlet and the outlet of the hollow impeller with single phase flow (gas flow only)
2. The inlet with the single phase flow ( gas flow) and the outlet with two phase flow (Both gas and liquid)
3. The both the inlet and the outlet with two phase flow (gas flow and liquid flow).

The systems other than the type one is involved with gas and liquid flow either at the outlet or at both inlet and the outlet. Hence these are less amenable to theoretical analysis with the present status of knowledge and it has been noticed that the investigations made towards this end is also rare.

The first category gas inducing systems are technically simple and easy to analyze using the fundamental principles. There is a reasonable volume of literature available in which these system behaviors were creatively modeled the and these models were found effective in predicting the systems in terms of hydrodynamics and various kinds of transport properties. In this paper an effort has been made to review the literatures which are theoretically sound and technically being close to the real systems of the type one and the outcomes are summarized to bring an insight into the hydrodynamic behavior of the gas inducing mechanically agitated contactors.

## 2.Hydrodynamic Characteristics of the GIMACs

It is evident from the literatures that various investigators employed systems with a wide range of geometrical features for studying about the gas inducing mechanically agitated contactors. One of the most recent work employed a novel L-shaped tube bundles inserted to the sold shaft to study about the gas holdup of the gas inducing systems[14]. Despite of this broad range in geometrical features, a common nature of the similar hydrodynamic characteristics has been essentially observed in different systems. The above statement may be appropriate in justifying the fact that the investigators have applied of the common fundamental platform for the analysis of the most of the systems. The general hydrodynamic characteristics of the GIMACs have been subjected to the detailed analysis with respect to various types of the systems differing in the geometrical features.

### 2.1 Critical gas induction speed.

The critical gas induction speed is strictly refers to the rotational speed of the impeller. In order to develop a model for predicting the critical impeller speed, it is essential to establish a relationship between the linear velocity of the orifice and the hydrostatic pressure head. This relation can be brought by using Bernoulli's equation and can be given as follows after neglecting the frictional pressure losses.

$$d\left(\frac{\rho U^2}{2}\right) + dP = 0 \qquad (1)$$

In the case of the gas induction is through the open tips of the impeller then the impeller tip velocity will be considered. This relation is depending on many factors like impeller geometry, number of the impeller blades, physicochemical properties of the system etc. It was succeeded in measuring the local pressure around a hollow impeller and establishing a model which relates the local pressure during the gas flow with the static liquid heads using the equation (1) and can be given as[7],

$$P' = \frac{h_S - h_L}{\frac{V^2}{2g}} \qquad (2)$$

This is the very first attempt to understand the gas induction process in a basic level with the knowledge of the local orifice pressure. The prime drawback of the above model is that the equation (2) will not relate the impeller speed and the local pressure hence the critical impeller speed cannot be determined from this equation.

The extension of the above model was successful in relating the $U$ with the impeller speed as[2],

$$U = (1 - K)2\pi NR \qquad (3)$$

where the $K$ is the slip factor between impeller and fluid. They have also defined the pressure coefficient in terms local pressure and head space pressure as,

$$C_p(\theta) = \frac{(P_o + \rho_L g S) - P(\theta)}{\frac{1}{2}\rho_L U^2} \qquad (4)$$

The pressure coefficient or the pressure loss coefficient is essentially the function of the shape of the blade and the orifice location and is calculated from the potential gas flow theory. The substitution of equation (3) in (4) and rearranging results,

$$P(\theta) = (P_o + \rho_L g S) - \frac{1}{2}\rho_L C_p(\theta)[2\pi NR(1 - K)]^2 \qquad (5)$$

At the critical impeller speed $P(\theta)$ equals $P_o$ and $N = N_{CG}$ . So the rearrangement of the equation (5) yields an expression in terms of critical speed as,

$$N_{CG} = \sqrt{\frac{gS}{\left[2C_p(\theta)(1 - K)\pi R\right]^2}} \qquad (6)$$

Even though the above equation is theoretically strong in establishing the required relation of critical gas induction speed with the other known variables, the measured local pressure field has not directly been related to the impeller geometry such as shape of the blade, width of the blade, impeller diameter and bottom clearance. A correlation for predicting critical gas induction speed was also found significant and can be given as,

$$\frac{N_{CG}{}^2}{g h_L}\left(\mu/\mu_w\right)^{-.011} = 0.21 \qquad (7)$$

This was successful in predicting the critical speed with 10% accuracy with respect to their system composed of an inducing impeller with hollow pipes[1]. Another model also can be given for predicting the critical speed of gas induction as follows[3],

$$N_{CG} = \frac{\sqrt{2(g h_S - h_{f1})}}{\pi d_d K} \qquad (8)$$

The above model has been developed by studying a system in which the improvements were made for the higher gas induction rates at reduced impeller speeds which could be led to the lower power consumptions. In a typical design improvement in their model, each of the gas outlets on the impeller was extended to an increased length of 95 mm by using 8mm diameter pipes and the gas outlets were the end opening of the pipes. According to the above equation the critical speed of gas induction is inversely proportional to the $d_d$ and directly proportional to the $h_s$. The above equation can be rewritten in the following form by considering the energy loss in the turbulent field is negligible compared to the potential energy term $g h_s$ ,

$$N_{CG} = \frac{\sqrt{2gh_S}}{\pi d_d K} \qquad (9)$$

It is evident from the above literature that the geometrical features of the impeller and the vessel influences the critical speed gas induction by a large extend. The improved impeller design by extending the distance of the orifice from the centre of the impeller and providing a downward inclination of the orifice increased the blade slip factor. This has resulted in a decrease of the critical impeller speed of gas induction and which can be justified by the equation (8) or (9). A baffle clearance provided at the bottom of the vessel was also capable in arresting the tangential movement of the liquid at the bottom to certain extend and resulted in the increment of the relative velocity of the impeller and the liquid. This contributed towards the increase in the slip factor as a consequence the critical impeller speed reduced. The equation (9) also relates the critical gas induction speed to the liquid head above the orifice in the absence of the gas flow and is clear from the above equation that the submersion depth of the orifice is directly proportional to the critical impeller speed. The extension of the single orifice impeller model to the multiple orifice impeller systems with $n_o$ of orifices on the impeller blade surface has resulted the modification of the equation (6) to the following form[12]

$$N_{C_i} = \sqrt{\frac{gh}{2[\pi r_i (1 - K_i)]^2 [C_{p_i}(\theta) - 1]}} \qquad (10)$$

For $i$=1,2……$n_o$. The critical speed of the gas induction is inversely proportional to the radial distance of the orifices from the vertical axis of the impeller. Therefore the orifice which is located farther from the impeller axis will have the lower critical speed of gas induction. In the most of the given equations the effort has not been made to relate the critical speed to the impeller geometry such as shape of the blade, width of the blade, impeller diameter and clearance.

### 2.2. Rate of gas induction

The measurement of local pressure around the hollow pipe impeller made possible to correlate the local pressure empirically to the gas induction rate, using orifice discharge coefficient. It was assumed in this exercise that the dominant pressure loss along the path is across the orifice. The following equation was proposed for the estimation of the rate of gas induction through a single orifice.

$$Q_O = C_o A_o K_1 \left( \frac{\rho_L}{\rho_G} \left( C'_p(\theta) U^2 - 2gh_s \right) \right)^{1/2} - K_1 K_2 \qquad \textbf{(11)}$$

The constants $K_1$ $K_2$ was introduced to the equation as correction terms for satisfying the condition at zero gas flow rate at the critical impeller speed. An analogy with fully turbulent flow in a circular pipe with uniform cross section was assumed in the development of the above equation and is hardly expected to satisfy the gas flow in the induction process. In addition to this, the constants present in above equation is supposed to vary in accordance with the variations in the geometrical features of the impeller and the hollow shaft like, shape of impeller blade, location and diameter of the orifice, diameter of the hollow shaft, blade angle and so forth. As of these reasons, the above model was not efficient in the prediction of the gas induction rates of most of the practical systems. The increase in the diameter of the gas outlet orifices increased the rate of gas induction has been reported. The increase in the diameter from 0.8 mm up to 12mm increased the induction rate about 250%. This increment in the gas induction was happening certainly at the expense of the larger bubble size.

In the gas inducing systems, above the critical speed the gas will be induced at a rate which is dependent on the impeller speed, vessel geometry, impeller geometry, the orifice position on the blade surface and orifice submersion depth. Further to this an equation has been proposed for gas induction rate which was trying to accommodate the effect of the above factors and can be given as follows[2],

$$Q_1G = C_1o\, A_1o \sqrt{(\blacksquare((\rho_1(L\,(1-\epsilon)\,)/\rho_1 G\, + \epsilon)@C_1p\,(\theta)[2\pi RN(1-K)\dagger 2 - (2\rho_1 L\, gS)/\rho_1 G\,))} \qquad \textbf{(12)}$$

As being an extension to the model as given in the equation(2) the above equation gives an accurate prediction of the gas induction rate even at higher rotational speeds and also exhibit slight offsets when the

rotational speed is fairly low. Since it has modeled on the basis of better assumptions in defining the system, this model was successful with systems widely varied. It is noticeable that from the above equation that the presence of the pressure loss coefficient - a solid function of the geometrical features of the system - makes the gas induction rate a strong dependent on the geometrical features of the system.

It has been found that the pressure differential generated at the aerated condition is lower than the unaerated condition . This is due to the lowering of the bulk fluid density at the impeller region due to the low dispersion of gas. As a result a decrease of the generated liquid velocity occurs and hence the induction rate decreases. If the mean density of the liquid is maintained as high as equivalent to the liquid density by creating higher dispersion rate of the solute gas in the working fluid, a higher rate of the gas induction can be accomplished. Another model also has been put forward an equation for predicting the gas induction rate which can be given as follows[3],

$$Q_G = S\sqrt{\left[\frac{\rho_L(1-\varepsilon_g)}{\rho_g}+\varepsilon_g\right]\left[(\pi d_d NK)^2+2h_{f1}-2h_g\right]-2h_{f2}} \quad (13)$$

The model exclusively developed by the study of gas inducing systems which had been used the modified impeller system for higher gas induction at lower rotational speeds. The improvement accomplished by this system modification can be clearly justified using the above equation. The above equation was successful in predicting the gas induction rate of the system used for his investigations under various conditions with various system combinations constituted by different impeller geometries, submersion depths and range of impeller rotational speeds. The experimental result of the work also highlight that the common nature of the dependence of the submersion depth on the gas induction rates. The higher submersion depths had always resulted in the lower induction rates.

The experimental works revealed that the gas induction rate increases for the larger the radial distance of the orifice location from the centre of the hollow shaft. This is because of the increase in driving force of gas induction with respect to the increment in the radial distance of the orifice location[8]. The gas induction rate is also increased as the number of orifices on each blade increases. These are the outcomes of their experimental work on the system with T= 0.5 m and D is 0.25 at various combinations like, impeller clearances of T/3 and 2T/3, PBTD with different blade angles of 30,45, and 60 degrees. Each blade were with 6 orifices in 3mm diameter and possible to keep the holes open and closed. The internal diameter of the hollow shaft was 20m. Slip factor for the individual orifices was found at a range of $0.7\pm$ 0.01. Increased blade angle has increased the rate of gas induction. This was because of the decrease in the slip factor as a result the increase in flow separation in the vessel that would increase the pressure driving force. Higher power consumption was observed from the higher blade angles due to the increase in the drag force. Another model also can be used for predicting the gas induction rate for the multiple orifice systems[10,12] and it is the extension of the model given in the equation(12)

$$Q_{o_i} = \frac{4\pi U_i\sqrt{C(\theta)}\left(r_{b_i}^3 - r_i^3\right)}{3\left(r_{b_i}-r_i\right)} \quad (14)$$

The above equations accommodate all the factors which are responsible for the pressure loss in a gas induction process through a multiple orifice impeller system. For the single orifice the surface tension and the frictional pressure losses are negligible as compared with the orifice pressure drop[2]. But in the case of the multiple orifice systems, the frictional pressure drop becomes more important due to the higher rate of the gas induction. In the above work, the system had the following specifications. Tank diameter is 0.45m with baffles. The six bladed concave impeller having a diameter of 0.154 m with four orifices on each blade with same angular locations at the different radial distances. The radial distance between each orifice is 7-8 mm and the orifice diameter is 1mm. The distance of 7-8mm will ensure that the interactions between the bubbles are negligible. It has been found from the experimental work that the use of 4 orifices than a single one increased the rate of gas induction by three times. The modified model was successful to predict the gas induction rate within the 20% of the experimental value. Even though the models given in the equations (12) and (14) can be used for an approximate estimation of the gas induction rate, the both models have not made an effort to make a

fundamental relation between the local pressure coefficient to the blade geometry or the impeller speed. But these equations can be effectively used for the design and optimization of the gas inducing impeller systems.

In the multiple impeller orifice systems, the gas inducing characteristics of the each orifice were found similar[13]. The values of the pressure loss coefficient are approximately equal for each orifice along the blade. (3.1-3.4 is the observed range variation of $C_p$ for the first 3 orifices). The Cp value falls with the increase in the radial distance which was complying with the previous observations[2]. The predictions of the model given in equation (14) for the gas flow rate shows good agreement with the experimental data except for the orifice at the impeller tip. This was due to the three dimensional flow patterns at this region. The gas induction rate was under predicted by model for this orifice by around 40%. The developed model indicates that the orifice which is farthest from the impeller hub contributing the highest rate of gas induction. This is due to the highest relative velocity of the liquid over the orifice. Increase in the number of outlet orifices makes certain increase in the gas induction rates. The model over predicts the value of the induction rate as the number of orifices increases. This investigation, it was found around 10% over prediction in the case of the 2 orifices and 20% in the case of 4 orifices. The important point is that the r/R ratio of various orifices was not varied and tested in this work (only in the range of 0.6 to 0.9). So care should be taken in the event of extrapolation is practiced for other system combinations using this model.

A curve fitted empirical correlation for the maximum value of the ratio $\frac{Q_g}{V_L}$ has also found significant in predicting the gas induction rate[1].

$$\left[\frac{(Q]_g}{V_L}\right) = (2.36 \times 10^{-4}) N^{1.53} \left(D/T\right)^{1.83} n_p{}^{0.26} \qquad (15)$$

The above correlation is only a data fitting exercise and is not holding any physical significance with respect to the system.

The importance of a secondary impeller in the enhancement of the rate of induction has been found in various literatures[1,6,8,14] . The secondary impeller can increase the pressure reduction the liquid hence complementing the increased distribution and uniform dispersion of the gas bubbles. So the induction rate may be increased. According to the literatures, the prevailing approaches can be only used for the rational design of the same at right now and the future possibilities in the research of the gas inducing impellers may be a systematic investigation of the effect of blade shape, number of blades, and orifice location on the gas induction rate on the basis of power consumption. The resulting data will be providing a basis for the selection of an appropriate geometry for the gas inducing impellers.

### 2.3. Power consumption

The power consumption in stirred vessels and equipment contribute significantly to the utility cost. The power drawn by the impeller is consumed for various purposes, like generation of the bulk liquid flow, generation of turbulence, dispersion of the induced gas, solid suspension, heat transfer, mixing etc. So the power consumption had a direct influence on the performance of a gas inducing mechanically agitated contactors. Most of the investigators so far agreed that the power consumption on the gassed state is lower than the ungassed state. The reduction in the power consumption can be explained by two reasons.

a) Cavity formation behind the impeller blades make more streamlined liquid flow around the impeller which will reduce the drag and causing in the reduction of power consumption.
b) Recirculation of a certain amount of the gas in the vessel that will reduce the average density of the working fluid. Thus the power consumption is reduced.

The model for power consumption given in equation (16) is considered as one of the earliest model for predicting the same[1]. The following assumptions are made in the development of the same.

- The density of the gas liquid dispersion was assumed to be the weighted mean of the densities of the gas and the liquid.

- The ratio of the liquid flow generated by the impeller to the rate of gas induction was related to the gas flow number through an empirical relationship obtained by experiments on a centrifugal pump.

$$\frac{P_G/P_L}{1 - P_G/P_L} = \frac{\rho_G}{\rho_L}\left[\alpha\left(1/N_{QG}\right)^n + \beta\right] \qquad (16)$$

The relevance of the above equation cannot be justified for all the cases because in a gas induction process, there will be liquid flow as well as the induced gas flow through the liquid. By this reason itself the gas induction is different from the operation of the centrifugal pump. The power consumption of the gas inducing impeller can also be given by the following correlation[5], which is

$$P_G = C\left(P_L^2 N D^3/Q_G^{0.56}\right)^{0.45} \qquad (17)$$

This work reveals that the value of the constant C is strongly related to the number of the gas inducing pipes and has a sound dependence on the gas induction rate at lower gas flow rates. The equation (17) can be considered as a more generalized form of correlation as compared to the correlation given in the equation (16). The investigations in the hollow pipe impellers and resulted in correlating the gassed power consumption with the following equation[1].

$$P_G/V_L = 0.62N^{3.44}\left(Q/V_L\right)^{-0.31}\left(d/D\right)^{4.48} n_P{}^{1.07} \quad (18)$$

The investigations in four and six hollow pipe impeller and a hollow disk impeller have also been found. They have correlated the gas induction rate with Reynolds number and Froude number and can be given as follows

$$\frac{N_{QG}}{N_{QG^\infty}} = 1 - exp\left(-C R_e{}^{c_1} Fr^{c_2}\right) \qquad (19)$$

For a concave bladed impeller, the drop in the power consumption at the gassed condition is less compared to the other impeller geometries by 10%[13]. The power consumption is approximately independent of the number orifices in the blade surface. The analysis in the power consumption in PBTD with the blade angles of 30, 45 and 60 degrees for the submergence values of $T/3$ and $2T/3$ (T=0.5m) made evident that the gas induction rate increases with the increase in the gassed power consumption[9]. In general the power consumption studies are not so wide and elaborate in the GIMACs and most of the studies contributed the results in the form of correlations. These correlations have not tested in the wide range of applicability in terms of different designs and various sizes of equipments. So it is advisable that care should be taken in the event of the application of these correlations beyond the experimental ranges used by the investigators. The gas hold up characteristics of the gas inducing system with a novel L shaped tube impellers suggest a directly proportional relationship of power consumption with rotational speed of the impeller[14].

### 2.4. Pressure driving force for gas induction

There are four kinds of energy dissipation in a gas induction process and they are; pressure drop in the hollow pipe or shaft, orifice drop, kinetic energy imparted to the liquid for the formation of the bubble and work done for overcoming the surface tension for the formation of the bubble at the orifice. The total pressure drop of the induction process can be given as the sum of the gas side pressure drop and liquid side pressure drop.

$$\Delta P_T = \Delta P_G + \Delta P_L \qquad (20)$$

The gas side pressure drop accounts the pressure drop due to the passage of the induced gas in the gas pathway (hollow pipe) and the orifice pressure drop. Whereas the liquid side pressure drop account the amount of energy dissipated in the form of work done against the surface tension and the impartation of the kinetic energy to the gas bubbles.

$$\Delta P_G = \Delta P_P + \Delta P_o \qquad (21)$$

$$\Delta P_L = \Delta P_\sigma + \Delta P_{KE} \qquad (22)$$

The pressure loss in the work against the surface tension imparted to the liquid bubble surface can be given by the following equation.

$$\Delta P_\sigma = {}^{\sigma}/_{r_b} \qquad (23)$$

The pressure lose due to the kinetic energy imparted to the liquid during the bubble formation process can be given as follows,

$$\Delta P_{KE} = \frac{3Q_o{}^2\rho_L}{32\pi^2 r_b{}^4} \qquad (24)$$

The improvement of the above equation to the following form by accounting the velocity field generated by the expansion of the spherical bubbles[13].

$$\Delta P_{KE} = \frac{3Q_o{}^2\varphi\rho_L}{32\pi^2 r_b(r_b{}^3 - r_o{}^3)} \qquad (25)$$

The $\varphi$ in the above equation is the constant derived from numerical integration of the velocity field generated by the expanding spherical bubble. This term accounts for the effect of impeller blades and relative cross-flow on the kinetic energy transfer. The value of the same is approximately 1.5.

The total pressure drop can be given as follows[2,10],

$$\Delta P_T = \frac{1}{2}\rho_L(C_P - 1)[2\pi Nr(1-K)]^2 - \rho_L g h \qquad (26)$$

This model account the pressure drops of the all kinds which given above and can be applied to number designs with a certain amount of success. The previous models failed to predict the pressure driving force of the gas induction process as Evans model done due to fact that those were not included with the kinetic energy term. For the single orifice the surface tension and the frictional pressure losses are negligible as compared with the orifice pressure drop, which typically accounts around one third of the total pressure driving force and the kinetic energy term[2]. The kinetic energy term is always the largest among of all these constituents of the pressure driving force.

Through the measurement of the pressure profiles in the liquid behind the impeller blades, it has been found that the pressure driving force reached a maximum slightly off the blade surface in the wake region behind the blade. Locating the orifice at such a location increased the air induction rate by 5 to 10% as compared to the orifice located on the blade surface. Through the measurement of the gas and liquid side pressure resulted in the following correlations[9],

$$\Delta P_G = C_G 0.5\rho_G \left({}^{Q_G}/_{A_o}\right)^2 \qquad (27)$$

$$\Delta P_L = C_L Q_G{}^A \left(\frac{H}{S}A_o\right)^B (2\Pi Nr)^C \qquad (28)$$

These two correlations were showing good agreement with the experimental values and hold good for wide range of the blade angles of the PBTD. The second correlation indicates that the effect of the gas induction rate on the liquid side pressure drop is less than that of the rotational speed of the impeller. This is due to the subsequent formation and breakage of the gassed cavities behind the impeller blades, that is the change in the hydrodynamic conditions behind the impeller blade. The subsequent drop and rise in the ${}^{P_G}/_{P_o}$ in the power characteristics curve which is plotted with ${}^{P_G}/_{P_o}$ vs the Areation number $\left({}^{Q_G}/_{ND^3}\right)$ in a gas flow range of 0.0035 to 0.0087$m^3$/s ascertains the change in the hydrodynamic conditions behind the impeller blades. The

power spectra analysis also made by the authors at a gas flow rate of 0.006m$^3$/s and impeller speed range of 4 to 6 rps. This also strongly supports the subsequent formation and breakage of the gassed cavities behind the impeller blades. In the above work, the value of $C_G$ in equation (27) varied according to various orifice combinations. But it was found that for each combination, the value was same for different PBTD blade angles of 30, 45 and 60. The predicted value of the gas induction vs the calculated value of gas induction also shown a good agreement at both the submersion depth at all used blade angles and orifice combinations. Care should be taken while using the above correlations of (27) and (28) because the authors have derived the same by only analyzing PBTD of blade angles of 30, 45 and 60 at two submergence values of T/3 and 2T/3.

Further modifications to the model given in equation (14) were proposed in order to make an extension of this the model to accommodate the effect of multiple orifices on a single blade[13]. The equation for the total pressure driving force can be given as,

$$-\Delta P_{T_i} = \Delta P_P + \Delta P_{CH_i} + \Delta P_{O_i} + \Delta P_{\sigma_i} + \Delta P_{KE_i} \qquad (29)$$

Here there is a new terms introduced that, $\Delta P_{CH_i}$ which will account the pressure drop due to the change in gas velocity along the hollow blade. This assumption is valid only in the case of the multi orifices on the blade surface. The above equation is also derived on the basis of the assumption that the frictional losses are same for all the orifices irrespective of its varying radial distance from the impeller axis. According to above literature the pressure loss due the variation in the gas velocity can be found with the help of the Bernoulli's equation and can be given by,

$$\Delta P_{CH_i} = \frac{\rho_L}{2}\left(\frac{4}{\pi d_{CH}^{\,2}}\right)^2\left[\left(\sum_{j=i-1}^{n_o} Q_{o_i}\right)^2 - \left(\sum_{j=i}^{n_o} Q_{o_i}\right)^2\right] \qquad (30)$$

For $i = 1, 2, \ldots n_o$

The frictional pressure drop which accounts all the losses of the gas flow from the gas inlet in the head space to the first orifice on the blade and can be given by,

$$\Delta P_P = c' + c'' Q_T + c''' Q_T^{\,2} \qquad (31)$$

Where the $Q_T$ is the overall volumetric gas induction rate through all orifices and $c'$, $c''$, and $c'''$ are the empirical constants depending on the nature of the gas pathway along the hollow shaft and the blade and these will be determined experimentally. The pressure loss across the orifice can be presented by the following equation.

$$\Delta P_{o_i} = \frac{\rho_G Q_{o_i}^{\,2}}{2\, C(\theta)_i^{\,2} (\pi r_i^{\,2})^2} \qquad (32)$$

for $i = 1, 2, \ldots n_o$. $C(\theta)_i$ is the empirical pressure loss coefficient for the orifice at the radial distance $r_i$ on the blade surface. The pressure drop due to the work done against the surface tension at the bubble surface can be given by

$$\Delta P_{\sigma_i} = \frac{2\sigma}{r_{b_i}} \qquad (33)$$

The radius of the bubble should be considered as the radius of the orifice at the critical impeller speeds in order to avoid the same term indeterminate at the critical speeds. The determination of the kinetic energy imparted to the bubble during its formation can be found on the basis of the potential flow model for an expanding sphere in the point of contact with a plane wall and can be expressed as the following relation[10].

$$\Delta P_{KE_i} = \frac{3\beta Q_{oi}^{\,2}}{32\pi^2 r_{bi}(r_{bi}^{\,3} - r_{oi}^{\,3})} \qquad (34)$$

For i= 1,2,. . . $n_o$

In the case of the multiple orifice systems, the frictional pressure drop become more important due to the higher rate of the gas induction but it is still only 15% of the total. But the pressure drop due to the variation in the gas velocity through the hollow blade channel is generally negligible i.e., the term constitute to the equation (32).

### 2.5. Bubble formation, gas holdup and bubble size

The above three related intimately in the case of gas inducing mechanically agitated contactors. The bubbles formed from the induction are getting sheared at the impeller region and they coalesce in the region of lower pressures. The equilibrium between these two decides the size of the bubbles. The photographic investigation techniques revealed that a cavity formation is taking place behind the impeller blades and the bubble generation is from these cavities[1]. The stator blades used in his study did not show any influence on the size reduction of the bubbles but increased the number of bubbles generated and also modify the flow patterns. His study also suggests that the use of two impellers fitted relatively closer can increase the energy consumption in the cavities and this will improve the formation of the bubbles. The size of the bubbles can be found by using the following equation by assuming isotropic turbulence and no coalescence of the bubbles taking place[1].

$$d_B = J\left(\frac{\sigma^{0.6}}{\rho_L{}^{0.2}\left(P_G/V\right)^{0.4}}\right) \qquad (35)$$

A modified form of the above equation also been proposed by considering the bubble coalescence by including the holdup term[1].

$$d_B = J\left(\frac{\sigma^{0.6}}{\rho_L{}^{0.2}\left(P_G/V\right)^{0.4}}\right)\varepsilon_G{}^{\delta} \qquad (36)$$

The above both equations shows that the bubble diameter is inversely proportional to the power consumption so the interfacial area is directly proportional to the $\left(P_G/V\right)^{0.4}$.

The bubble formation in a liquid cross flow can be divided into three regimes i.e, Single bubbling, Pulse bubbling and Jetting. The different parameters which decide the bubble formation regime are liquid cross flow velocity, gas velocity through the orifice and diameter of the orifice[6]. Single bubbling is normally observed at reasonably low gas flow rate through the orifice and the formed bubbles are characterized by their regular production and nearly the spherical shape with uniform sizes. They detach very close to the orifice. In the single bubbling regime the bubble diameter can be predicted by the following equation.

$$d_b = \left(\frac{16 r_o \sigma}{C_d U^2 \rho_L}\right)^{0.5} \qquad (37)$$

At comparatively higher flow rates, pulse bubbling will be predominant. Formation of the increasingly non spherical bubbles and its detachment away from the orifice also observed with elongated neck joining the bubble to the orifice. In the bubble formation 2 or 3 bubbles joins together to produce a single or an agglomerated bubble There are several models are available or proposed to describe the pulse bubbling regime. But they are limited to a particular extend due to some reasons as follows,

- Very low liquid cross flow velocities typically less than 4 m/s in GIMAC induces very small non spherical bubbles
- Assumption of spherical bubble growth.

At very high gas velocities the continuous gas jet is formed from the orifice and this gas jet subsequently breaks up at a small distance from the orifice result in the production of small irregular shaped small bubbles. The mean size of bubbles formed by this process can be predicted by a jet break up model confirmed by the experimental work and can be given as follows[1],

$$d = 2.4\left(Q_o/U_o\right)^{0.5} \qquad (38)$$

In general in gas inducing systems, it is difficult to predict the bubble generation regimes because of the difficulty in observing the system and is considered as one of the major limitation in predicting precise bubble generation regimes. The gas inducing impeller systems will not operate in the single bubbling regime. It will be mix of all these three regime .so with any one of these models; we can't predict the bubble sizes simply.

A model also has been proposed, that predicts the gas flow rate in terms of the total bubble formation time can be given in terms of the bubble detachment radius and total time for the bubble formation as follows[13].

$$Q_o = \frac{4\pi\left(r_d^3 - r_d^3\right)}{3}\frac{1}{t_d} = \frac{4\pi\left(r_d^3 - r_d^3\right)}{3}\frac{UC_p{}^{0.5}}{(r_d + r_o)} \qquad (39)$$

The bubble produced in the above investigation was approximately 2-2.5mm in diameter are formed from 1 mm diameter orifice. Slight increase in the bubble size with the increase in the impeller speed has been observed in the experimental work. The bubble size distribution is independent of the impeller speed in a range of 4-8 rps and in this range the mechanism of the bubble formation being the same[13].

**Gas holdup.**

The fractional gas holdup in terms of gas flow number, Froude number and the Reynolds number hollow pipe impellers with four and six pipes can be correlated as follows[4],

$$\epsilon_G = BF_r{}^{b_1}R_e{}^{b_2}N_{QG}{}^{b_3}\left(D/S\right)^{b_4} \qquad (40)$$

It reported that the multiple impellers can increase the gas dispersion characteristics in the GIMAC so it will increase the gas holdup[6]. The study also reveals that the increase in the inter impeller distance reduces the gas holdup. The investigation of the effect of submersion depth and combination of a secondary impeller on the gas holdup of the gas inducing system with novel impeller type revealed that the addition of a secondary impeller has a significant effect on the gas holdup of the system[14]. In addition to this the closer inter-impeller clearance of 50 mm can create a higher holdup than of a 100 mm or a 150 mm. This may be because of the higher relative velocity generated by the impeller system and effective dispersion and distribution of the induced gas bubbles in the liquid. The above authors also reported a higher gas holdup with the lower submersion depth.

## 3. Conclusion

The most important features of the gas inducing mechanically agitated contactors (GIMACs) are lower power consumption and enhanced recycle of the solute gas. GIMACs can be classified in to various types on the basis of the fluid flow through the impeller inlet and outlet. It has been found that most of the cited literatures were dealing with the impeller systems with the only gas flow though the both inlet and outlet in the gas inducing segment. There are several models which are predicting the various hydrodynamic characteristics of the gas inducing mechanically agitated contactors. The first established work in its kind had been done for studying single orifice impeller blades. The model developed for this has been extended or improved later with respect to various aspects like critical impeller speed, gas induction rate, power consumption etc. These modifications of the models were the results of impartation of better and solid assumptions in defining the systems and the latter models were more successful in predicting different hydrodynamic behaviors of the gas inducing systems. Further to this, the models which were evolved for the analysis of multi orifice impeller systems. These investigations and the resulted expressions gave better clarifications for the pressure differential generating when the induction process is on the way. The models which are developed for estimating the pressure differential by means of gas and liquid phase pressure differential have been successful in the respective focus. The most important point observed that the developed models for the induction process were inefficient in establishing perfect relation of corresponding hydrodynamic behaviors with the various system geometries. These models can only be used for an approximation of the parameter under the investigation and a

cautioned extrapolation can only be practiced. The developed models were also successful in analyzing the mechanisms of bubble formation and ejection. Efficient models which are relating the local pressure and the impeller design has to be established and this is the area where more emphasis has to be given by the current researchers. As the local pressure being a very important factor in the gas induction process, those relations can facilitate the rational design of the gas inducing impellers and optimization of the gas inducing systems. The authors of the cited literatures had limited their work with the maximum vessel size of around 0.5m. The investigations in the larger gas inducing systems are also necessary to understand the way of the system behaves under a scale up process. These aspects can be addressed more easily by the application of various computational tools.

**Nomenclature**

$A_o$ = Area of the orifice, $m^2$
$C$ = Constant in the equation 17
$C_d$ = Orifice drag coefficient. Dimensionless
$C_G, C_L, A, B, C$ are the empirical constant for the equations 27 and 28.
$C_o$ = Impeller orifice discharge coefficient
$C_p(\theta)$ = Pressure loss coefficient or pressure coefficient
$C_{pi}(\theta)$ = Pressure loss coefficient for orifice at a radial distance $r_i$ on the blade surface.
$D$ = Impeller diameter, m
$d$ = Diameter of the pipe, m
$d_B$ = Diameter of the bubble, m.
$d_{Ch_i}$ = Diameter of the hollow channel along the blade surface, m.
$d_d$ = Diameter to the orifice in the impeller, m
$F_r$ = Froude number based on submergence.
$g$ = Acceleration due to gravity $m/s^2$
$H$ =Total liquid height, m
$h_L$ = Liquid head outside the orifice, m
$h_s$ = Liquid head above the orifice in the absence of gas flow, m
$J$ = Constant in the equation 35 and 36
$K$ = Slip factor between impeller and the fluid or speed loss coefficient
$K_i$ = Slip factor for the orifice at a radial distance $r_i$.
$K_1$ = Dimensionless empirical constant to correct the pressure loss in equation (11)
$K_2$ = Empirical constant used in equation (11), $m^3/s$
$N$ = Impeller rotational speed, rps
$N_{CG}$ = Onset gas induction speed, rps.
$N_{ci}$ = Critical impeller speed for the gas induction for the orifice at a radial distance $r_i$ on the blade surface.
$N_{GQ}$ = Gas flow number
$n$ = constant in the equation (16)
$n_p$ = Number of impeller pipes or blades
$P$ = The Combined pressure, $N/m^2$
$P_G$ = Power drawn by the gassed impeller, W
$P_L$ = Power drawn by the impeller in the liquid, W
$P_o$ = Head space pressure, $N/m^2$
$P[\theta]$ = Pressure at any angular location at the impeller blade, $N/m^2$
$P_i(\theta)$ = Pressure at the any angular location for orifice at a radial distance $r_i$ on the blade surface, $N/m^2$
$P'$ = Dimensionless pressure
$\Delta P_T$ = Total pressure drop through the hollow impeller passage, $N/m^2$
$\Delta P_{Ti}$ = Total pressure driving for orifice at orifice at a radial distance $r_i$ on the blade surface, $N/m^2$
$\Delta P_G$ = Gas side pressure drop, Pa.s
$\Delta P_{KE}$ = Pressure loss due to imparted kinetic energy, Pa.s
$\Delta P_{KEi}$ = Pressure loss due to imparted kinetic energy to the bubbles for the orifice at a radial distance $r_i$ on the blade surface., $N/m^2$

$\Delta P_L$ = Liquid side pressure drop, Pa.s
$\Delta P_P$ = Pressure drop in gas path, Pa.s
$\Delta P_{Pi}$ = Pressure drop in gas path for the orifice at a radial distance $r_i$ on the blade surface., Pa.s
$\Delta P_o$ = Pressure drop across orifice, N/m
$\Delta P_{oi}$ =Pressure drop across the for the orifice at a radial distance $r_i$ on the blade surface., $N/m^2$
$\Delta P_\sigma$ = Pressure drop due to work done against surface tension, Pa.s
$\Delta P_{\sigma i}$ = Pressure drop due to work done against surface tension for the orifice at a radial distance $r_i$ on the blade surface., $N/m^2$
$\Delta P_{Ch_i}$ = Pressure drop due to the change in the gas velocities along the hollow blade for the orifice at a on the blade surface., $N/m^2$
$Q_G$ = Gas induction rate $m^3/s$
$Q_o$ = Gas induction rate through a single orifice, $m^3/s$
$Q_{o_i}$ = Gas induction rate through the orifice at a radial distance $r_i$ on the blade surface, $m^3/s$
$R$ = Radius of the impeller, m
$R_e$ = Reynolds number.
$r$ = Orifice distance from the impeller axis, m
$r_b$ = Radius of the gas bubble, m
$r_{b_i}$ = Radius of the bubble detached from the orifice at a radial distance of $r_i$ on the blade surface, m.
$r_d$ Bubble detachment radius, m
$r_o$ = Outlet orifice radius, m
$S$ = Submersion depth of the impeller orifice in the liquid, m
$T$ = Tank diameter, m
$t_d$ = Total time required for the bubble formation, s.
$U$ = Liquid velocity upstream of the orifice relative to the orifice velocity, m/s
$U_i$ = Liquid velocity upstream of the orifice relative to the orifice velocity for the orifice at a radial distance $r_i$ on the blade surface, m/s
$U_o$ = Liquid velocity over the orifice relative to the orifice velocity, m/s
$V$ = Velocity of the impeller tip, m/s
$\alpha$ = Impeller pumping number
$\beta$ = Constant in the equation (16)
$\delta$ = Constant in the equation 36
$\varepsilon$ = Fractional gas hold up in the working medium
$\varepsilon_G$ = Fractional gas holdup
$\theta$ = Attacking angle of the impeller blade.
$\mu$ = Viscosity of the liquid, Pa.s
$\mu_w$ = Viscosity of water, Pa.s
$\rho$ =The Density of the working fluid $kg/m^3$
$\rho_G$ = Gas density, $kg/m^3$
$\rho_L$ = Density of the liquid, $kg/m^3$
$\sigma$ = Surface tension of liquid, $N/m^2$
$\varphi$ = Constant derived from numerical integration of the velocity field generated by the expanding spherical bubble
PBTD = Pitched blade turbine down flow.

## References

1. Ashwin W. Patwardhan and Jyeshtharaj B. Joshi., Design of Gas-Inducing Reactors, Industrial Engineering and Chemistry Research Journal,1999, 38, 49-80.
2. Evans.G.M, Rielly.C. D, Davidson, J. F, Carpenter. K. J., Hydrodynamic Characteristics of a Gas-Inducing Impeller, Proceedings of the 7th European Conference on Mixing, Kiav, Brugge, 1991,18-20, 515-523.

3. Fan Ju, Zhen-Min Cheng, Jian-Hua Chen, Xiao-He Chu, Zhi-Ming Zhou and Pei-Qing Yuan, A novel design for a gas-inducing impeller at the lowest critical speed, Chemical Engineering Research and Design Journal, 2009, 87,1069-1074.
4. Joshi, J. B., Modifications in the Design of Gas Inducing Impellers, Chemical Engineering Communication Journal, 1980, 5 (1-4), 109-114.
5. Joshi, J. B and Sharma, M. M., Mass Transfer and Hydrodynamic Characteristics of Gas Inducing Type of Agitated Contactors, Canadian Journal of Chemical Engineering and Technology, 1977, 65, 683-95.
6. Kaliannagounder Saravanan, Vishwas D. Mundale, Ashwin W. Patwardhan, and Jyeshtharaj .B. Joshi, Power Consumption in Gas-Inducing-Type Mechanically Agitated Contactors, Industrial and Engineering Chemistry Research Journal, 1996, 35,1583-1602
7. Martin, G. Q ,Gas-Inducing Agitator, Industrual and Engineering Chemistry Process Design and Development Journal. 1972, 11, 397-404.
8. Raidoo, A. D, Raghav Rao, K. S. M. S, Sawant.S. B and Joshi. J. B., Improvements in a Gas Inducing Impeller Design, Chemical Engineering Communication Journal, 1987, 54, 241-64.
9. N. A. Deshmukh, S. S. Patil and J. B. Joshi, Gas induction characteristics of hollow self-inducing impeller, Chemical Engineering Research and Design Journal, 2006, 84(A2), 124–132.
10. Rielly, C. D, Evans.G.M, Davidson.J. F and Carpenter. K. J, Effect of Vessel Scale-up on the Hydrodynamics of a Self-Aerating Concave Blade Impeller, Chemical Engineering Science Journal, 1992, 47, 3395 3402.
11. Saravanan. K, Mundale. V. D, and Joshi. J. B, Gas Inducing Type Mechanically Agitated Contactors, Industrial Engineering and Chemistry Research Journal, 1994, 33, 2226-2241.
12. S.E. Forrester and C.D. Rielly, Modeling of increased gas capacity of self inducing impellers, Chemical engineering science Journal, 1994, 49, 5709-5718.
13. S.E Forrester, CD Rielly and KJ Carpenter, Gas inducing impeller design and performance characteristics, Chemical engineering science Journal, 1998, 56, 603-615.
14. C. Gomadurai, K. Saravanan, Eldho Abraham and N. Deepa, Hydrodynamic Studies on Air Inducing Impeller Systems, International Journal of Chem Tech Research, 2014, 6, 4471-4474.

*****